Proc. Nat. Acad. Sci. USA
Vol. 71, No. 10, pp. 3866–3868, October 1974

Equilibrium Sedimentation of Turnip Yellow Mosaic Virus

(magnetic ultracentrifuge/preferential interaction/Donnan effect/molecular weight)

J. H. McGEE, D. W. KUPKE*, W. GODSCHALK*, AND J. W. BEAMS

The Department of Physics, and the *Department of Biochemistry, The University of Virginia, Charlottesville, Va. 22903

Contributed by Jesse W. Beams, July 25, 1974

ABSTRACT **Sedimentation equilibrium was achieved with turnip yellow mosaic virus at low speeds (600 rpm) in a magnetic ultracentrifuge. The experiments were carried out in the newly installed constant-speed rotor, equipped with automatic control and an electromagnetic drive. A particle mass of 5.55×10^6 daltons was calculated for the virus at vanishing concentrations, in essential agreement with the earlier results using the more tedious procedure with a freely coasting rotor. In order to interpret the observed departure from ideal behavior (nonassociating conditions), preferential interaction experiments were carried out by magnetic densimetry. These showed that a strong Donnan effect exists at pH 7, which contributed $>10^3$ times more to the nonideality than did the excluded volume effect. A net negative charge of about 3.5×10^3 per particle was estimated at this pH.**

In order to achieve an equilibrium distribution of very large macromolecules, such as viruses, in a centrifugal field, the rotor speeds must be comparatively small (e.g., 10 rev/sec) and be constant (or varied at precisely known rates). In our previous attempts with turnip yellow mosaic virus (TYMV), the magnetic ultracentrifuge was used with the rotor coasting freely in the vacuum chamber. It was necessary, however, to make tedious extrapolations to equilibrium from quasi-equilibrium states because the rotor speed was constantly decreasing (about 1% per day). In the present study with TYMV the rotor was automatically driven electromagnetically at constant speed (10^{-3}% or $\pm 10^{-4}$ rev/sec) without heating or rotor hunting for the entire experiment (1). Also, the rotor may now be accelerated (or decelerated) to an operating speed electromagnetically, thus eliminating the mechanical drive system wherein a spindle had to be withdrawn through an oil gland after attaining operating speed. This, in turn, eliminates all oil from the vacuum chamber and provides for cleaner optical systems (an interferometer was used in this work).

The results for the particle mass of TYMV by use of the speed-controlled instrument essentially confirmed our previous result, i.e., 5.5×10^6 daltons (unpublished), with the coasting rotor. In addition, it was possible to better evaluate the degree of nonideality. Because the net charge on the virus was not known at the solvent conditions used (pH 7), preferential interaction experiments were performed by magnetic density measurements; these showed that the net charge, $|Z|$, must be very large in order to account for the observed excess chemical potential. The molecular properties of TYMV have been reviewed and discussed in detail by Kaper (2), and the results of x-ray analyses have been described by Klug *et al.* (3). Briefly, this isometric particle resembles an icosahedron with 20 hexagonal and 12 pentagonal faces having an extreme diameter (anhydrous) of 29 nm (30 nm for the interparticle distance in crystals). The capsid, or protein shell, consisting of 32 morphological units, is believed to contain 180 identical protein subunits; the amino- acid sequence (189 residues per subunit), indicating unusual hydrophobicity, was reported recently (4). About one-third of the mass of the virus is RNA (5), which appears to be interwoven to some extent among the protein subunits. From these observations, and with the average specific volumes of the protein and the RNA (6), it is highly unlikely that the virus is compact throughout; a comparatively large space into which solvent may penetrate is probably enclosed by the virus (7). The degree of interaction of the RNA and protein is not clear, however, nor the degree of this effect on the net charge.

Abbreviation: TYMV, turnip yellow mosaic virus.

EXPERIMENTAL

TYMV was obtained from the U.S. Dept. of Agriculture, Beltsville, Md., and is the same strain used in the many studies by J. M. Kaper and in the previous reports from our laboratories. The virus was grown on Chinese cabbage leaves for 21 days at 20° in an artificially lighted growth chamber (by Dr. Kaper). Virus was isolated from the minced leaves with Mg-bentonite suspensions (8). The top component (RNA-less protein capsids) was removed by means of density gradient centrifugation (27,000 rpm for 3 hr in a Spinco SW-27 rotor) in aqueous sucrose in which the weight fraction of sucrose initially varied from 0.14 to 0.56 vertically down the tubes. These and subsequent centrifugations were carried out in a buffer medium consisting of 75 mM KCl–6.75 mM K_2HPO_4–4.75 mM KH_2PO_4, pH 7.0 (ionic strength = 0.1). The virus band drawn from the sucrose gradient was dialyzed against the buffer. This was followed by three cycles of sedimenting the virus out at $105,000 \times g$ for 1 hr, and of resuspending the virus pellet in fresh buffer in order to remove smaller fragments of RNA and protein. The final suspension was dialyzed against the buffer in boiled cellophane bags and was then passed through a washed Millipore filter (pore size = 0.8 μm) with filter pad. The amounts of capsid and of RNA and protein fragments in the samples used for the equilibrium studies were judged to be at or below the level of detection by velocity sedimentation analysis in a Spinco model E instrument, wherein a combination of schlieren and ultraviolet absorption optics was used.

All concentrations used in sedimentation and density experiments were based on a consistently applied dry weight procedure. Weighed water solutions (200–400 mg) of the virus were gently evaporated under nitrogen at 40°, then

dried under reduced pressure at 105° to constant weight (corrected for air buoyancy); the latter weight was an extrapolated value to the time the samples were removed from the vacuum chamber at the temperature of the analytical balance. Variations in the dry weight fraction of different samples of a stock solution was less than 1 part in 800. An extinction coefficient of 8.59 ml/mg (20°) at 261.5 nm was determined and used for the concentration analyses after correcting for scatter by subtracting from the observed absorbance, $A_{261.5}$, the quantity, $(320/261.5)^2 \times A_{320}$, where the subscript numerals are wavelengths. The salts used had no detectable absorption at these wavelengths. Density determinations were made with a magnetic densimeter (9), and refractive increments were measured with a Brice-Phoenix differential refractometer.

The apparent weight-average molecular weight, M_a, for each equilibrium experiment was obtained from the limiting slope of plots of ln c against r^2 according to the relation

$$(d \ln c/dr^2)^{c=c_a} = (\omega^2/2RT)(\partial\rho/\partial c)_\mu{}^{c=c_a} M_a \qquad [1]$$

where c is the concentration of unsolvated virus (g/ml) at radius r from the rotation axis, ρ is the density, ω the angular velocity, a the meniscus, and μ refers to constant chemical potential of the nonvirus components. The temperature, T, was held at 278°K and the rotor speed at 10.000 rev/sec for all experiments. Any redistribution of salts at equilibrium, therefore, arises essentially from interactionn with virus so that Eq. [1] is applicable (see ref. 10). The concentration ratios, c_b/c_a, at equilibrium, where b is the bottom and a the meniscus of the solution column (<3 mm), ranged from about 1.7 to nearly 1.9 for the various initial concentrations, c_0, at this rotor speed. The limiting slopes were virtually coincident with a linear least-squares fit through the data points. Equilibrium was established by plotting the Archibald function, $(rc)^{-1}\, dc/dr$, against r (11) at intervals during the runs until a ± 1% correspondence to that equilibrium definition was achieved; this degree of correspondence was at the limit of resolution of the interference optical system currently used. Nonideality, but not polydispersity, was indicated in experiments at the high concentrations by the Archibald procedure. The isopotential density derivative, $(\partial\rho/\partial c)_\mu$, in this solvent medium was obtained by preparing weight dilutions of the dialyzed virus solution with dialysate for the magnetic density measurements according to the method outlined by Kupke and Beams (12). The density was found to be a linear function of c for the virus over the span of concentrations used to a high level of confidence (correlation coefficient, r, was better than 0.99999); hence, the same value for this derivative (0.335) was applied in all runs at any r under the assumption that the effect of pressure at this low speed was negligible. The measurements for c along r in the centrifuge, by interferometry, were proportional at all concentrations to the definition by which the density increments were evaluated. In our case the refractive increments, $(\Delta n/c)$, were determined on dialyzed solutions and dialysate, as was $(\partial\rho/\partial c)_\mu$, using the same dry-weight definition of c for both.

RESULTS

The values of M_a obtained in the individual sedimentation equilibrium experiments were plotted as $M_a{}^{-1}$ against c_0 (initial concentration) and also against $(c_b - c_a)/2$ and extrapolated by linear least-squares fitting to $c = 0$ in order to compare the values of M ($c = 0$) and the slopes by the two

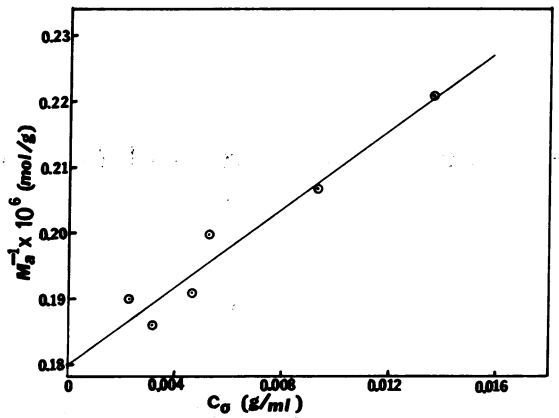

FIG. 1. Reciprocal of the weight-average apparent molecular weight versus the initial concentration, c_0, of turnip yellow mosaic virus.

procedures. Both methods yielded virtually the same value for the particle mass at $c = 0$, i.e., 5.55×10^6 and 5.56×10^6 daltons, respectively. These values are in essential agreement with the more recent data of other kinds (see ref. 2). A plot of $M_a{}^{-1}$ against c_0 is shown in Fig. 1. Fujita (13) has shown that this type of projection may be used for virial expansion under the conditions used here (short solution columns, low speeds, and monodisperse sedimenting solute). Neglecting the higher terms in this expansion, the value of the second virial coefficient was calculated to be 2.97×10^{-6} ml·moles·g^{-2}. The corresponding value for the initial slope when using the average concentration over the cell was 2.91×10^{-6} ml·mole·g^{-2}, which is the value for the excess chemical potential (designated herein as 2B) (see ref. 13). The correlations from linear, least-squares fittings to each kind of plot showed no difference in linearity (r = 0.9752 compared with r = 0.9759). Thus, neglect of the higher terms in the virial expansion seems appropriate. The scatter of the data at the lower concentrations is believed to result from the limit of precision of the present optical system when only a few fringes are measured.

The value for the second virial coefficient (equivalent to 2B) is not satisfied by merely accounting for the excluded volume effect of nonassociating isometric macromoles (if Donnan effects are negligible). B is given by $4\phi/M$ (ml·moles·g^{-2}) for noninteracting spheres (see ref. 14), where ϕ is the apparent specific volume of the sphere. The excluded volume, u, (ml/g) is 8ϕ for such spheres. Since $\phi = \bar{v} = 0.673$ ml/g for the virus (see below), $u = 5.384$ ml/g, so that $B = u/2M = 0.49 \times 10^{-6}$ ml·mole·g^{-2}. Hence 2B by hard sphere exclusion is about 33% of that observed in Fig. 1. As a rule of thumb, however, globular proteins exhibit about one-third more exclusion than hard spheres as a result of solvation and of small departures from sphericity (14). Thus, a value of 0.65×10^{-6} ml·mole·g^{-2} is more appropriate (44% of the observed nonideality). Since the virus has been shown to possess spherical symmetry in crystals (3) and exhibits a behavior in solution that is compatible with that for solvent-filled spheres (7), the existence of a substantial Donnan effect must be suspected if the observed value of 2B is correct. Unfortunately the net charge, $|Z|$, of the particle in this solvent medium is not known, and sedimentation studies at higher ionic strengths were not carried out. To account for the discrepancy between B and u, a net charge of about 100 per particle is required

(ref. 14, equation 14–24), which is much too small (i.e., $|Z| < 2$ per 10^5 g) if the isoelectric point is at pH 3.75 (15). Measurement of the preferential interaction, however, showed a positive preference for the salts, suggestive of a strong Donnan effect. The difference in molality of the salts (lumped together as component 3) in the virus solution relative to that in the dialysate is a measure of this interaction, which is conveniently carried out by density measurements (see ref. 16). For preferential interaction in terms of the excess (or deficient) grams of component 3 per gram of dry virus, ξ_3^0, at osmotic equilibrium, we have at vanishing virus concentration (superscript zero).

$$\xi_3^0 = [(\partial\rho/\partial c)_\mu^0 - (\partial\rho/\partial c)_m^0]/(1 - \bar{v}_3'\rho') \qquad [2]$$

where m denotes constant molality of the salts, primes to dialysate quantities (i.e., $\rho' = \rho^\circ$), and $\bar{v}'_3$ is the partial specific volume of the salt mixture (0.5083 ml/g) in the absence of the virus at the salt concentration used in the centrifuge. (If ξ_3^0 is negative, the excess water, ξ_1^0, is obtained by substituting $\bar{v}_1'$ for $\bar{v}'_3$). So long as the macromolecule concentrations are determined concurrently on the same preparation for both the ispotential and isomolal series of density measurements, the values of ξ can be obtained with useful accuracy. The linear density-concentration slopes, however, ought to be obtained with a confidence where $\mathbf{r} = 0.99999$, which can be achieved in routine practice. A value of 0.325 was found for $(\partial\rho/\partial c)_m$ independent of c (thus, $\phi = \bar{v}$), which is close to, but significantly lower than, that for $(\partial\rho/\partial c)_\mu = 0.335$. Hence $\xi_3^0 \cong +0.020_4$ excess grams of salt per gram of virus, which in our experience is probably accurate to no worse than $\pm 25\%$ at this small a value. Since component 3 is predominantly KCl, the preferential number of moles of this salt (if the phosphates can be neglected) per mole of virus is nearly 1500. Applying Scatchard's general relation for the excess chemical potential, B, for two diffusible components and one nondiffusible component at osmotic equilibrium (ref. 17, equation 34) and converting to the units used here, the negative contribution to nonideality arising from preferential interaction is very closely 1.5×10^3 times greater than the positive, excluded volume contribution. [The term containing the former contribution also included a small effect from the concentration and activity coefficient of the KCl; the latter coefficient was taken from Harned and Owen (18).] Thus, the Donnan effect (a positive contribution) must also be virtually 1.5×10^3 times greater than the excluded volume effect according to the Scatchard relation, even if the observed value of 2B is only roughly correct. Calculation of the net charge on this basis yields $|Z| \cong 3500 \pm 700$ per particle. Since this value of $|Z|$ was arrived at only in terms of the order of magnitude, no confidence should be placed on the numerical value itself. It may be noted, however, that about 6600 sodium or potassium ions have been found to be associated with the particle at neutral pH (19). Also, from the RNA and amino acid composition of the virus, somewhat over 6000 net negative charges per particle can be counted at pH 7 *if* there is no interaction between the RNA and protein; a substantial amount of interaction, however, is likely.

We are indebted to Mr. T. E. Dorrier for extremely careful analytical measurements and to Dr. J. M. Kaper for providing virus, encouragement, and very valuable advice. This report was drawn in part from a dissertation (J.H.M.) at the University of Virginia in partial fulfillment of the requirements for the Ph.D. degree. This work was supported by grants from the U.S. Department of Health, GM-12569, and GM-11630, and from the National Science Foundation, GB-27331 and GP 31721.

1. McGee, J. H., Beams, J. W. & Kupke, D. W. (1974) *Rev. Sci. Instr.*, in press.
2. Kaper, J. M. (1969) in *Molecular Basis of Virology*, ed. Fraenkel-Conrat, H. (Reinhold Book Corp., New York), pp. 1–133.
3. Klug, A., Longley, W. & Leberman, R. (1966) *J. Mol. Biol.* **15**, 315–343.
4. Stehelin, D., Peter, R. & Duranton, H. (1973) *Biochim. Biophys. Acta* **293**, 253–265.
5. Kaper, J. M. & Litjens, E. C. (1966) *Biochemistry* **5**, 1612–1617.
6. Kupke, D. W. (1966) *Fed. Proc.* **25**, (Symposia & Reports), 990–992.
7. Kupke, D. W., Hodgins, M. G. & Beams, J. W. (1972) *Proc. Nat. Acad. Sci. USA* **69**, 2258–2262.
8. Dunn, D. B. & Hitchborn, J. H. (1965) *Virology* **25**, 171–192.
9. Senter, J. P. (1969) *Rev. Sci. Instr.* **40**, 334–338.
10. Casassa, E. F. & Eisenberg, H. (1964) *Advan. Protein Chem.* **19**, 287–395.
11. Archibald, W. J. (1947) *J. Phys. Colloid Chem.* **51**, 1204.
12. Kupke, D. W. & Beams, J. W. (1972) in *Methods in Enzymology*, eds. Hirs, C. H. W. & Timasheff, S. N. Vol. 26, (Academic Press Inc., New York), pp. 74–107.
13. Fujita, H. (1962) *Mathematical Theory of Sedimentation Analysis* (Academic Press Inc., New York).
14. Tanford, C. (1961) *Physical Chemistry of Macromolecules* (Wiley & Sons, Inc., New York).
15. Markham, R. (1951) *Faraday Soc. Disc.* **11**, 221–227.
16. Kupke, D. W. (1973) in *Physical Principles & Techniques of Protein Chemistry*, ed. Leach, S. J. (Academic Press Inc., New York), part C pp. 1–75.
17. Scatchard, G. (1946) *J. Amer. Chem. Soc.* **68**, 2315–2319.
18. Harned, H. S. & Owen, B. B. (1950) *The Physical Chemistry of Electrolyte Solutions* (Reinhold Publ. Corp., New York), 2nd ed.
19. Johnson, M. W. (1964) *Virology* **24**, 26–35.